

# Selection of Near-Fault Pulse Motions for Use in Design

**C.P. Hayden, J.D. Bray, N.A. Abrahamson & A.L. Acevedo-Cabrera**

*University of California, Berkeley, CA, USA*



## **SUMMARY:**

Earthquake ground motions in the near-fault region can have intense, double-sided pulses in the velocity-time series that can be damaging to structures. Velocity pulses often result from the effects of forward-directivity (i.e., rupture propagation toward the site). The relative contribution of pulse-type motions to the overall seismic hazard should be considered when selecting records in a suite of design ground motions for a site in the near-fault region. This study classifies 390 records as pulse or non-pulse motions using a new classification scheme. A straightforward model is developed to estimate the proportion of pulse motions as a function of closest site-to-source distance and the epsilon of the seismic hazard. This proportion can then be used to estimate the number of pulse-type motions to include within a suite of design ground motions for use in time-history analysis to represent properly the relative contribution of pulse motions to the seismic hazard.

*Keywords: Ground Motion, Forward-Directivity, Near-Fault, Pulse, Velocity*

## **1. INTRODUCTION**

Earthquake records at small site-to-source distances often have different characteristics than those recorded at larger distances. Sites in the near-fault region may be influenced by the effects of forward-directivity (FD: rupture towards the site) or backward-directivity (BD: rupture away from the site). Forward-directivity often results in early arriving, large double-sided pulses in the velocity-time series.

These intense velocity pulse motions can affect adversely the seismic performance of structures (e.g., Anderson and Bertero, 1987; Hall et al., 1995; Alavi and Krawinkler, 2000). The period of the pulse in relation to the fundamental period of the structure also greatly affects structural performance (Anderson and Bertero, 1987). However, these large pulses do not always occur, even for sites located in the FD region. Other near-fault phenomena, including fling-step, basin edge effects, asperities along fault rupture and others, can produce intense pulses in the velocity-time series as well.

When selecting a suite of design motions for time-history analysis, it is the current state of practice in the United States (e.g., ASCE, 2005) that the magnitude, distance and other parameters are similar to those that control the hazard (e.g., obtained by a PSHA disaggregation by distance and magnitude). Unfortunately, there is a lack of guidance on how to include pulse-like motions into a suite of ground motions, even though the unique nonstationary characteristics of pulse-like motions can greatly affect structural performance (e.g., Anderson and Bertero, 1987; Alavi and Krawinkler, 2000). In this study, near-fault ground motions are classified as pulse or non-pulse motions using a new classification scheme. A straightforward equation is developed to estimate the occurrence of pulse motions in the near-fault region. This equation can be used with the results of a standard probabilistic hazard analysis (PSHA) to provide guidance on an appropriate number of pulse type motions to include in a suite for use in dynamic analysis of structures.

## **2. NEAR-FAULT GROUND MOTIONS**

When a fault ruptures toward a site, a rupture velocity that is slightly slower than the shear wave velocity results in the accumulation of seismic energy released during rupture (Somerville et al., 1997). This generally results in a large, double-sided pulse early in the velocity-time series. An opposite effect is observed in the backward-directivity region, where recordings generally have long durations but low amplitudes.

The radiation pattern of horizontally propagating shear waves (SH) has its maxima aligned along the strike of the fault and the observed pulse is the result of the superposition of these SH waves (Somerville et al., 1997). These SH waves are oriented normal to the fault and as a result the pulse is also oriented normal to the fault plane. Forward-directivity occurs for both strike-slip and dip-slip faults. In the case of strike-slip faults, sites located in the direction of fault rupture and at the end of the fault are typically most influenced by forward-directivity. For dip-slip faults, sites located up-dip of the rupture plane are generally most affected by forward-directivity.

Somerville et al. (1997) identify relatively simple parameters based on source-site geometry that can be used to estimate the effects of directivity on the response spectra, ratio of fault normal to fault parallel spectra, and duration. Later, Abrahamson (2000) recommended decreasing the maximum amount of long period spectral amplification estimated for the effects of FD for strike-slip earthquakes. Spudich and Chiou (2008) derive a more complex model to estimate the spatial variations of ground motions due to the effects of directivity. The Spudich and Chiou (2008) model offers several advantages over the older Somerville et al. (1997) model and estimates approximately half the amplification or deamplification due to directivity compared to the Somerville et al. (1997) model.

Directivity, fling-step, and other possible phenomena contribute to the characteristics of near-fault motions that are often quite distinct from more distant records. The differences are often most apparent in the velocity-time series. Bray and Rodriguez-Marek (2004) identify key parameters in the characterization of forward-directivity pulse motions including amplitude (PGV: peak ground velocity), velocity pulse period, and number of significant cycles. The amplitude of a pulse is often much larger than the median PGV as predicted from the Next Generation Attenuation (NGA) ground motion prediction equations (see Abrahamson et al., 2008 for a summary of the NGA models). The period of the pulse is also important to the seismic performance of structures. If the period of the pulse and fundamental period of the structure align, resonance can greatly increase the demands on a structure (Anderson and Bertero, 1987). A large number of significant cycles can be more demanding to a structure. Fortunately, in the case of forward-directivity, often only one or two significant cycles occur. Bray and Rodriguez-Marek (2004) used largely a qualitative classification scheme, based on their judgment, to develop a database of pulse motions likely caused by forward-directivity. This work was updated in Bray et al. (2009).

Recent work by Shahi and Baker (2011) also examines the occurrence of near-fault pulses by using a wavelet transform procedure (Baker, 2007) to extract pulse-like signals from velocity-time series and classify each recording as pulse-like or non-pulse-like. Their algorithm is quantitative but requires subjective thresholds which are unavoidable when classifying ground motions into binary categories. Using this database of pulse and non-pulse motions, they derive a model of the probability of observing a pulse using several parameters. Modifications are made to a traditional PSHA calculation to better account for near-fault ground motion characteristics.

## **3 PULSE MOTION CLASSIFICATION**

### **3.1 Dataset Selection**

In this study, a new classification scheme was developed to distinguish pulse motions from non-pulse motions. All ground motion data were from the 2005 NGA dataset (Chiou et al., 2008) used to develop

the NGA West ground motion prediction equations. Records with moment magnitudes greater than 6.0 and closest source-to-site distances ( $R_{RUP}$ ) less than 30 km were selected to include motions within and just beyond the near-fault region. Distance is an independent parameter in the derived model, and this threshold is not of major importance because beyond 30 km pulse motions are quite rare. Including more distant records in the regression could actually be detrimental to the fit of the model in the near-fault region.

Motions with moment magnitudes less than 6.0 were excluded for a variety of reasons. Events with magnitudes less than around 6.0 are not as likely to produce substantial forward-directivity, and there is also precedent for magnitude thresholds of around 6.0 from previous studies (e.g., Somerville et al. 1997). Larger magnitude events often control the hazard at a site, so excluding smaller events makes the model more applicable to the magnitude range of primary interest. The model was derived using events with magnitudes of 6.0 to slightly below 8.0 and as a result, care should be taken if trying to apply the model to events outside of this range.

Records with missing acceleration-time series for either horizontal component, unknown component orientations, or those not used by Abrahamson and Silva (2008) were excluded from the database in this study. Removing motions that were excluded by Abrahamson and Silva eliminated many inappropriate motions, including those from unrepresentative earthquakes, records taken inside certain types of buildings, duplicated stations and those missing key metadata (see Abrahamson and Silva, 2008b for a more in depth discussion of excluded motions). The Kobe 1995, Port Island (0 m) record (NGA# 1114) was removed as it was influenced by liquefaction. The Landers 1992, Lucerne (NGA# 879) record had two slightly non-orthogonal horizontal components (85 degrees) but for this study they were treated as orthogonal. In total, 29 motions were excluded due to the reasons mentioned. The resulting ground motion database contained 390 records from 35 earthquakes. A complete list of the 390 motions used can be found in Appendix C of NIST (2011). Appendix C of NIST (2011) also contains additional details regarding the proposed near-fault classification scheme and the derived models discussed in this paper.

## 3.2 Classification Scheme

### 3.2.1 Summary

This study identifies pulse motions as those with one or two intense cycles of motion in the velocity-time series. The classification scheme is carried out using MATLAB and allows the automatic classification of a large number of records in a short period of time. However, the authors recognize that no classification system is perfect, particularly a relatively simple method for classifying complex velocity-time series which can be extremely complex. For this reason, the authors allowed limited human intervention in the classification scheme if the algorithm did not appear to work well and a defensible reason for making the change was established. These manual modifications did not have a substantial effect on the final result; instead they merely refined the derived equation and provide a more reasonable database of pulse records for use in suites of ground motions (NIST 2011).

There are several key parameters used in the classification scheme, which require discussion. The first is the peak-to-peak velocity (PPV). As shown in Figure 1a, the PPV is the difference between the two peaks in one cycle of motion. PPV is used as a measure of amplitude in this study instead of PGV for several reasons. There are records where the orientation that maximizes the PPV is substantially more pulse-like than the orientation that gives the maximum PGV. The PPV is likely a better indicator of the demands placed on a structure because the PPV can range from slightly more than the PGV (a one-sided pulse) to slightly less than twice the PGV (a double-sided pulse). A double-sided pulse is expected to be more demanding to a structure than a single sided pulse with the same PGV. Additionally, many near-fault pulses are likely caused by forward-directivity and are expected to be double-sided pulses, so using a parameter that captures this phenomenon is desirable.

Another parameter used is the normalized cumulative squared velocity (NCSV). The NCSV at a given time increment is the sum of the squared velocity at each preceding time increment normalized by the

sum of the squared velocity at the end of the record. The NCSV of a record increases from 0% to 100% and increases rapidly during intervals of high velocity relative to the rest of the record. In Figure 1a, the NCSV increases rapidly during the pulse as expected. As a comparison, the NCSV in Figure 1b has a much more gradual increase that is indicative of a non-pulse-like motion. The uses of NCSV and PPV in the classification scheme are discussed later.

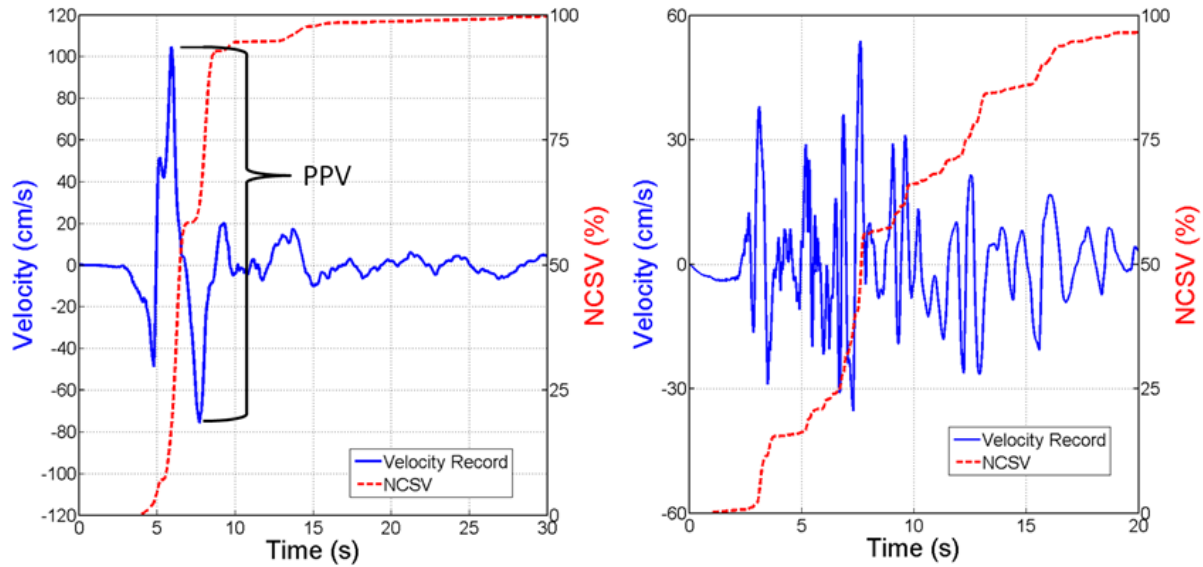


**Figure 1.** (a) Pulse-like recording of Imperial Valley 1979, El Centro Array #7 (NGA# 182). (b) Non-pulse-like recording of Imperial Valley 1979, Bonds Corner (NGA# 160).

### 3.2.2 Filtering

Filtering was applied to each time series using a low-pass, 3-pole, causal Butterworth filter to focus on the characteristics of the velocity-time series associated with the primary velocity pulse, which is in the long period range. This filtering also improves the consistency of the classification scheme. The pulse periods in this study varied from less than a second to over 6 seconds, so using a constant cutoff frequency for all records would be inappropriate.

An appropriate cutoff frequency was calculated for each motion. The predominant pulse period was estimated as the period with the largest ratio of the velocity spectra (5% damping) of the record to the median spectral velocity (from the NGA relationships). The record was then filtered using a corner period of one-third of the estimated period. Figure 2 shows an example of estimating the pulse period for the Imperial Valley 1979, Brawley Airport record. The solid line shows the ratio of the two spectra and reaches its maximum at a period of 4.65 seconds. A corner period of  $4.65/3 = 1.55$  seconds (a frequency of 0.645 Hz) is then used to filter the record. A more complete description of the process can be found in Appendix C of NIST (2011).

### 3.2.3 PPV pulse identification

The filtered, orthogonal components of the acceleration-time series were integrated to obtain velocity-time series and then rotated through all possible orientations at one degree increments. At each orientation, the largest PPV pulse is identified along with related parameters. The basic steps of the algorithm involve calculating the PPV, finding the number of cycles that have amplitudes exceeding 25% of the PPV (termed “significant cycles”), and calculating the amount the NCSV increases during the PPV pulse (termed NCSV difference). A more detailed process and associated definitions can be found in Appendix C of NIST (2011).

The NCSV difference is a good indicator of the pulse-like nature of a record. If the NCSV increases a large amount during the largest pulse of a record, it indicates that the pulse is substantially larger than

other cycles of motion in the record. The number of half cycles associated with the PPV pulse also indicates how pulse-like a record is. If a large number of half cycles are associated with the PPV pulse, the motion is less pulse-like and more similar to an ordinary motion.

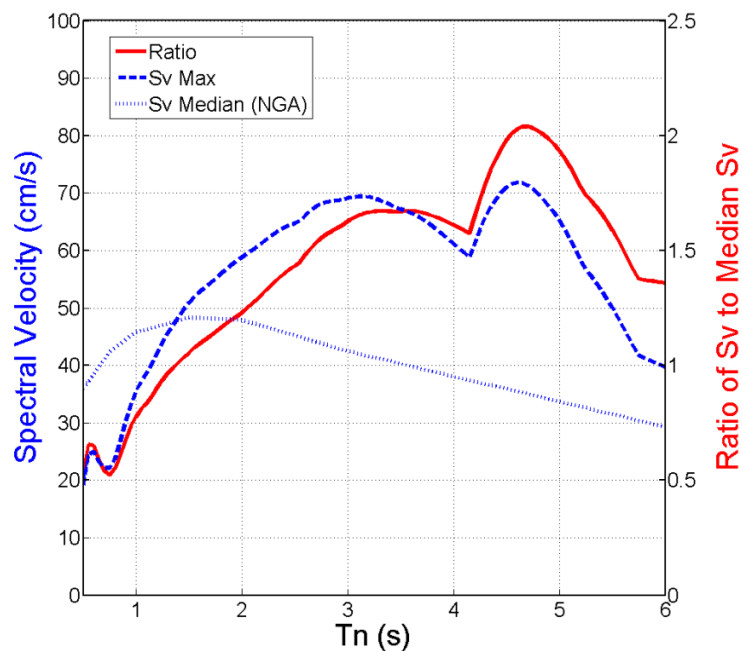


**Figure 2.** Example of period estimate used for filtering the Imperial Valley 1979, Brawley Airport record (NGA# 161).

### 3.2.4 Pulse classification score

In developing the classification procedure, the authors found that a composite score of several relevant factors provided a more robust classification method than using any single criterion alone. Additionally, it is also superior to using a series of discriminating thresholds. For example, requiring all pulse motions to have a NCSV difference greater than a set value and a number of significant cycles less than a second specific value will result in some motions being classified as a non-pulse because they were just slightly below the subjective threshold for one factor even though they far exceeded the threshold for the second factor. By scoring each record on two criteria and then combining the scores, a record that would have been just barely below one threshold but far above the second will actually score higher than a less pulse-like motion that happens to only slightly exceed the thresholds for both separate criteria.

The score for each factor ranged from 0% to 100%. In the NCSV difference category, motions with a NCSV difference above 0.7 scored 100%, while motions with an NCSV below 0.5 scored 0%. Motions between 0.5 and 0.7 received a score that transitioned linearly from 0% to 100%. For example, the Brawley Airport record had an NCSV difference of 0.635, so the NCSV score is 68%.

A similar taper was used in the score for number of significant cycles. Records with 1.5 cycles or less scored 100%, those with 2 cycles scored 50% and those with 2.5 or more cycles scored 0%. The Brawley Airport record had only one significant associated cycle, so it scored 100%. Combining the scores from the two factors with equal weighting (50% each) the overall pulse score was:  $0.5 \cdot 68\% + 0.5 \cdot 100\% = 84\%$ .

The scoring system described above was partly developed using the existing pulse databases of Shahi and Baker (2011) and Bray and Rodriguez-Marek (2004) to calibrate the scoring scheme. When binning the motions by NCSV or number of cycles and calculating the proportion of motions classified as a pulse of FD by the previous databases, it was clear that this proportion was highly dependent on NCSV or number of significant cycles. Using a logistic regression (appropriate for

binomial data), a similar trend resulted and agreed well with the binned data. As the NCSV difference increased, it was more likely that a given record had been classified as a pulse. As the number of significant cycles increased for a given record, it was less likely to have been classified as a pulse in the two existing classification databases. Several alternate parameters were considered that could also be used to classify pulses, but in this case a relatively simple combination of NCSV difference and number of significant pulses worked well. The specific thresholds and weights of the two categories were also calibrated in part by using these previous classifications.

The 390 motions were sorted by their pulse classification score, and a threshold of 60% in the score was selected by the authors to best mark the transition from pulse to non-pulse motions. Above 60%, most of the motions appeared visually pulse-like and below 60% most records seemed non-pulse-like. Again, in any classification scheme partitioning something as complex as a velocity-time series into binary categories, a subjective threshold is unavoidable. However, by using a threshold in the composite score, the effectiveness of the classification scheme was greatly improved compared to using thresholds on individual parameters.

An additional criterion was added that required motions to have a PPV greater than 25 cm/s to be considered a pulse. This minor requirement substantially improved the classification results, because there are records with low amplitude velocity-time series where a long period signal is picked up by the filtering algorithm, which would result in an unreasonable classification of the motion as being a near-fault pulse. This PPV threshold of 25 cm/s is set sufficiently low that it does not interfere with the classification of legitimate pulses.

Of the 390 records examined in this study, 87 records were classified as being velocity pulse motions, because they had scores greater than 60% required to be considered pulses. The classification scheme was supplemented by a subjective evaluation by the developers, because it was realized that the nuances of a record were not always captured by an automated classification scheme. For this reason, 7 of the 87 records were removed from the pulse category. Additionally, 8 records that did not have scores exceeding 60% were manually added to the pulse category. Thus, with the manual intervention, there were a total of 88 records classified as pulses.

### *3.2.5 Pulse period*

The pulse period of each record was estimated using the same method used to estimate the period of the pulse in the filtering process (Section 3.2.2). The only modification is that the motion is rotated to the max PPV orientation prior to calculating the spectral velocities. The pulse period is the period at which the ratio of the spectral velocity of the PPV pulse to the median spectral velocity from the NGA models is at a maximum. Several other methods of identifying the pulse period were also tested. These included using the period associated with the maximum spectral velocity, the ratio of the spectral velocity of the two orthogonal components, or the zero crossings of the pulse in the velocity-time series. However, these alternate methods did not prove to be as effective. The 88 pulse motions are grouped by the period of the predominant pulse in the velocity-time series and are provided in Appendix C of NIST (2011) along with other characteristics and plots of each pulse time-series. Engineers should select pulse records from the motions listed that cover the period range of interest for the structure being analyzed.

## **4 PROPORTION OF PULSE MOTIONS**

An investigation into the occurrence of pulse motions found that they are more likely to occur when the design ground motions parameter at the selected seismic hazard level is due to a high epsilon value (e.g., the deaggregation of the seismic hazard indicated that the design spectral acceleration at the period of the structure results from an epsilon value greater than one). Additionally, the likelihood of pulse motions occurring increases greatly as the source-to-site distance ( $R_{RUP}$ ) decreases. These trends are apparent even in the raw data scatter-plot of pulse and non-pulse motions shown in Figure 3.

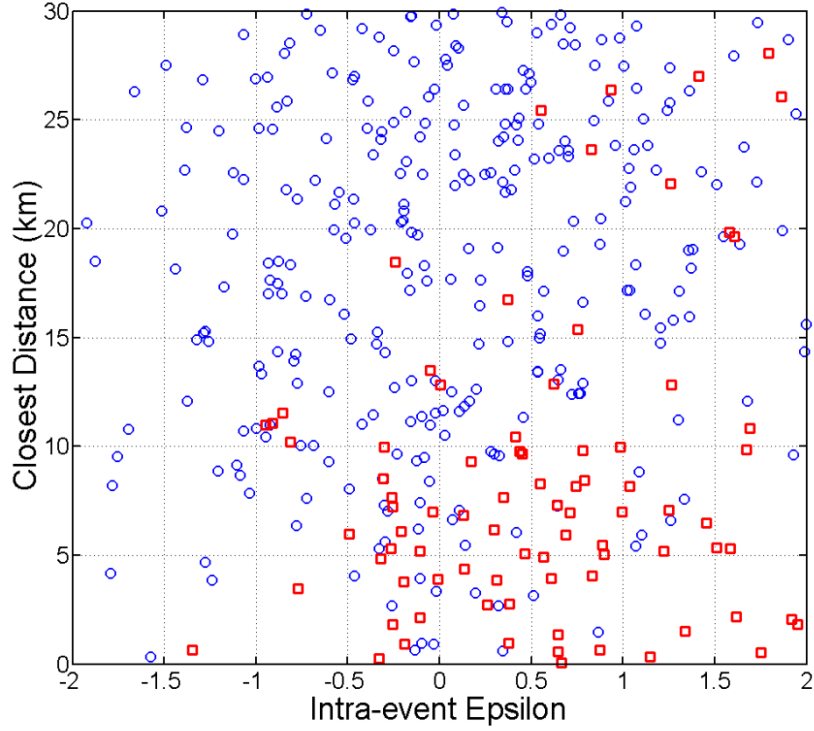


**Figure 3.** A scatter plot of 390 records with squares indicating motions classified as pulses and circles indicating non-pulse motions.

Intra-event (within-event) epsilon of PGV from Abrahamson and Silva (2008) was used to develop the initial model, but the final model was adjusted to use total epsilon. This was accomplished by normalizing the intra-event residual by the total standard deviation instead of the intra-event standard deviation to obtain an estimate of the mean total epsilon for future earthquakes with random event terms. This total epsilon is consistent with the total epsilon used by the engineer in practice. Therefore, the following relationships can be used directly with total epsilon. It is the recommendation of the developers that the PGV epsilon be used if available. If not available, using the epsilon of the spectral acceleration at the structural period is likely acceptable.

The model developed using logistic regression to capture the dependence of the proportion of pulse motions on epsilon and distance is displayed in Figure 4 for select distances. This figure is simply for visualization. In practice, the engineer should use the following equation with the epsilon ( $\epsilon$ ) of the design ground motion parameter and closest distance from the site to the source ( $R$  in km):

$$\text{Proportion of Pulse Motions} = \frac{\exp(0.891 - 0.188 * R + 1.230 * \epsilon)}{1 + \exp(0.891 - 0.188 * R + 1.230 * \epsilon)}$$

This relationship may be used by the engineer to estimate the number of ground motions within a suite of records that should be selected from among the 88 identified pulse motions to represent the proper contribution of pulse motions to the seismic hazard. For example, for the case wherein  $R = 10$  km and  $\epsilon = 1.5$  for the 5% damped spectral acceleration at the structural period of 1.2 seconds, the proportion of ground motions that should be pulse motions is 0.70. Thus, for this case, 5 records (i.e.,  $0.70 * 7 = 4.9$ ) of a suite of 7 records should be FD-pulse and pulse motions. The presented model can be used with the results of a probabilistic seismic hazard analysis by performing a disaggregation by distance and epsilon and using the values of these two parameters that control the hazard.

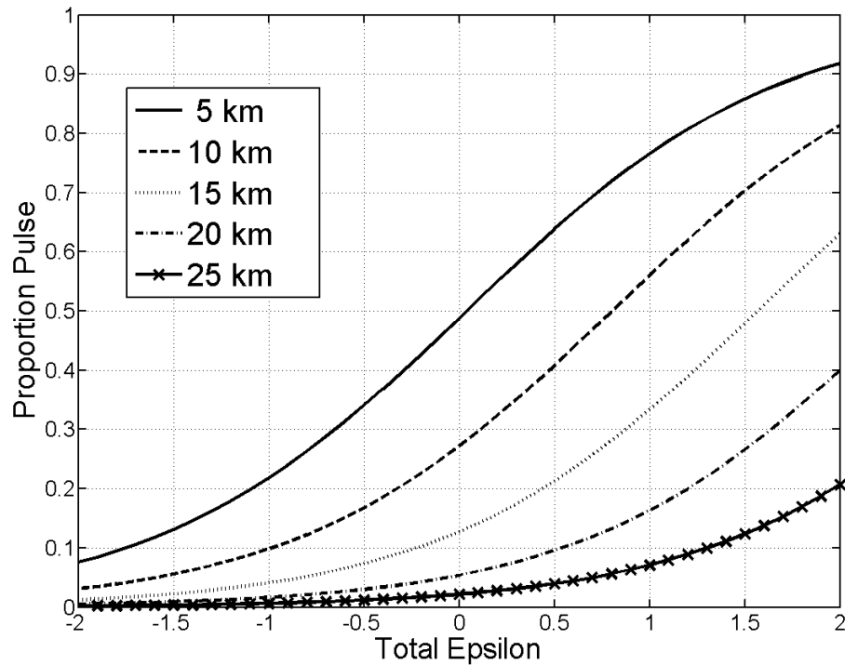


**Figure 4.** Model for estimating the proportion of pulse motions as a function of epsilon and distance.

The model was developed using pulses of all periods due to the limited data available and several other considerations. This may overestimate the likelihood of pulses when only interested in pulses with a specific period. For example, a pulse with a period of 6 seconds may not have a “pulse-like” effect on a building with a structural period of 1 second. One difficulty in addressing this issue is that there is not a clear transition when a pulse of a given period no longer has a “pulse-like” effect on buildings with varying fundamental periods. For example, a pulse with a period of 3 seconds will have a “pulse-like” effect on structures with periods of around 3 seconds, but it is not clear if it will be “pulse-like” effects on structures with periods of 1.5 seconds. Another issue is that the database is dominated by a few well-recorded earthquakes, most notably Chi-Chi with its aftershocks which make up nearly a third of the 390 records, and the current model gives equal weight to each recording. This is particularly concerning because magnitude has been shown to correlate with pulse period (Bray and Rodriguez-Marek, 2004; Shahi and Baker, 2011). For these reasons it is difficult to determine the proportion of pulses within specific period ranges. These issues warrant additional investigation in the future.

The engineer should select motions that best reflect the period range of interest in the structure being considered. With a limited number of design ground motions in the suite of motions (e.g., a suite of 7 motions is often used in practice and only a portion of these will be pulses), it is important to focus on the period range of interest of the structure. If many ground motions were to be used (e.g., more than 40 or so), then a more comprehensive suite of motions that captures all key earthquake scenarios including a wide range of pulse periods based on the potential near-fault earthquake scenarios could be used. Conventional good practices, such as selecting design motions that best represent the governing earthquake magnitude and distance, should be still followed.

If spectral matching is used, ideally, the motion should be spectrally matched using the concept of a conditional spectrum (Baker, 2011), because pulse motions contain high spectral ordinates within a narrow period range. Thus, spectral ordinates at other periods are likely to be below spectral acceleration values derived from a uniform hazard spectrum. However, traditionally a uniform hazard spectrum is used in earthquake engineering design practice, and for this case, it will be necessary to match the target spectrum over the specified period range (e.g.,  $0.2T - 1.5T$ , where  $T$  is the fundamental period of vibration of the structure). “Loose” spectral matching should be performed for

pulse-type motions so that the spectral ordinate at the period of the pulse is not larger than about 15% to 30% of the target spectral ordinate at this period and spectral ordinates at periods away from the period of the pulse are not less than about 10% to 20% of the target spectral values at these periods. Finally, the velocity-time series of the matched motion and the seed motion must be inspected to ensure that the nonstationary aspects of the seed motion are preserved in the matching process.

## 5 CONCLUSIONS

A new quantitative scheme was developed to classify near-fault motions as pulse or non-pulse motions. This scheme involves first filtering the record, calculating several parameters at all orientations, and then scoring motions based on two key ground motion parameters. The scheme was used to automatically classify 390 records with moment magnitudes greater than 6.0 and closest distances ( $R_{RUP}$ ) less than 30 km. The developers manually reviewed the results and adjusted the classification of a limited number of records, realizing that no numerically based classification procedure would be able to capture all the nuances of a record. In total 88 of the 390 records were classified as pulses.

Using the newly developed pulse database, logistic regression was used to derive an empirical model to estimate the likelihood of occurrence of pulse motions. The equation estimates the proportion of pulse motions as a function of epsilon and closest distance. A disaggregation by distance and epsilon from a probabilistic seismic hazard analysis can help estimate the appropriate values of distance and epsilon for use in the provided equation. Pulse motions are sorted by period in Appendix C of NIST (2011) to facilitate the selection of pulse motions to include in a suite of design earthquake ground motions for time-history analysis.

## ACKNOWLEDGEMENT

Financial support was primarily funded by the ATC-82 project through an ATC-CUREE joint venture sponsored by NIST/NEHRP. Additional funding is from a National Science Foundation Graduate Research Fellowship.

## REFERENCES

- Abrahamson, N.A. (2000). Effects of rupture directivity on probabilistic seismic hazard analysis. *Proceedings, Sixth International Conference on Seismic Zonation*, Palm Springs, CA, Nov. 12-15.
- Abrahamson, N., Atkinson, G., Boore, G., Bozorgnia, Y., Campbell, K., Chiou, B., Idriss, I.M., Silva, W., and Youngs, R. (2008). Comparisons of NGA ground-motion relations. *Earthquake Spectra*. **24:1**, 45-66.
- Abrahamson, N.A., and Silva, W.J. (2008a). Summary of the Abrahamson and Silva NGA ground-motion relations. *Earthquake Spectra*. **24:1**, 67-97.
- Abrahamson, N.A., and Silva, W.J. (2008b). Abrahamson and Silva NGA ground motion relations for the geometric mean horizontal component of peak and spectral ground motion parameters. *Final report prepared for the Pacific Earthquake Engineering Research Center*.
- Alavi, B., and Krawinkler, H. (2000), Consideration of near-fault ground motion effects in seismic design. *Proceedings, 12th World Conf. on Earthquake Engineering.*, Auckland, New Zealand.
- Anderson, J.C., and Bertero, V.V. Uncertainties in establishing design earthquakes. (1987). *Journal of Structural Engineering*. **113:8**, 1709-1724.
- ASCE. (2005). Minimum design loads for buildings and other structures. *ASCE/SEI 7-05*.
- Baker, J.W. (2011). Conditional mean spectrum: Tool for ground motion selection. *Journal of Structural Engineering*. **137:3**, 322-331.
- Baker, J.W. (2007). Quantitative classification of near-fault ground motions using wavelet analysis. *Bulletin of the Seismological Society of America*. **97:5**, 1486-1501.
- Boore, D.M., and Atkinson, G.M. (2008). Ground-motion prediction equations for the average horizontal component of PGA, PGV, and 5% -damped PSA at spectral periods between 0.01 s and 10.0 s. *Earthquake Spectra*. **24:1**, 99-138.
- Bray, J.D., and Rodriguez-Marek, A. (2004). Characterization of forward-directivity ground motions in the near-fault region. *Soil Dynamics and Earthquake Engineering*. **24**, 815-828.

- Bray, J.D., Rodriguez-Marek, A., and Gillie, J. L. (2009). Design Ground Motions Near Active Faults. *Bulletin of the New Zealand Society for Earthquake Engineering*, 42 (1), March, 8 pp.
- Campbell, K.W., and Bozorgnia, Y. (2008). NGA ground motion model for the geometric mean horizontal component of PGA, PGV, PGD and 5% damped linear elastic response spectra for periods ranging from 0.01 to 10s. *Earthquake Spectra*. **24:1**, 139-171.
- Chiou, B., Darragh R., Gregor N., and Silva, W. (2008). NGA project strong-motion database, *Earthquake Spectra*. **24:1**, 23-44.
- Chiou, B.S.J, and Youngs, R.R. (2008). Chiou-Youngs NGA ground motion relations for the geometric mean horizontal component of peak and spectral ground motion parameters. *Earthquake Spectra*. **24:1**, 173-215.
- Hall, J.F., Heaton, T.H., Halling, M.W., and Wald, D.J. (1995). Near-source ground motion and its effects on flexible buildings. *Earthquake Spectra*. **11:4**, 569-605.
- NIST. (2011). Selecting and Scaling Earthquake Ground Motions for performing response-history analysis. *Prepared by the NEHRP Consultants Joint Venture for the National Institute of Standards and Technology*.
- Shahi, S.K., and Baker, J.W. (2011). An empirically calibrated framework for including the effects of near-fault directivity in probabilistic seismic hazard analysis. *Bulletin of the Seismological Society of America*. **101:2**, 742-755.
- Somerville, P.G., Smith, N.F., Graves, R.W., and Abrahamson, N.A. (1997). Modification of empirical strong ground motion attenuation relations to include the amplitude and duration effects of rupture directivity. *Seismological Research Letters*. **68:3**, 199-222.
- Spudich, P., and Chiou, B.S.J. (2008). Directivity in NGA earthquake ground motions: Analysis using isochrone theory. *Earthquake Spectra*. **24:1**, 279-298.